Sheffield Hallam University

Influence of flowing fluid property through an elastic tube on various deformations along the tube length

NAHAR, Samsun <http://orcid.org/0000-0002-0930-5607>, DUBEY, Bipro <http://orcid.org/0000-0003-0396-9864> and WINDHAB, Erich J.

Citation:

Copyright and re-use policy

Influence of flowing fluid property through an elastic tube on various deformation along the tube length

Samsun Nahar, Bipro N. Dubey,* and Erich J. Windhab

Laboratory of Food Process Engineering, Swiss Federal Institute of Technology (ETH) Zurich, Schmelzbergstr 9, 8092 Zurich, Switzerland.

* Corresponding author contact: National Centre of Excellence for Food Engineering, Faculty of Science, Technology and Arts, Sheffield Hallam University, Howard Street, Sheffield S1 1WB, United Kingdom.

Email: b.dubey@shu.ac.uk, Phone: +441142254782

Abstract

The study of fluid flow characteristics in collapsible elastic tubes is useful to understand biofluid mechanics encountered in the human body. The research work presented here is aimed to thoroughly investigate the influence of both Newtonian and/or non-Newtonian fluid (low and high shear thinning) during steady flow through an elastic tube on various tube deformations, which enables understanding of the interaction between wall motion, fluid flow and intestinal transmembrane mass transfer as a crucial contribution to a mechanistic understanding of bio-accessibility/ bio-availability. It is observed that for a given steady volume flow rate, the tube is buckled from an elliptical shape to a line or area contacted two lobes as the critical external pressure is increased. The downstream transmural pressure is found to get more negative than that at the upstream as the outlet pressure decreased due to stronger tube collapse resulting in a reduced cross-sectional area. The experimental results depict that the tube cross-sectional area decreased by only about factor of one for PEG (Polyethylene Glycol) and about factor of six for both CMC (Carboxymethyl Cellulose) and PAA (Polyacrylamide) from the undeformed one under an applied external pressure of 105 mbar. The corresponding maximum velocity increased by a factor of two during steady flow of shear-thinning fluids. The shear-thinning behavior of both CMC and PAA solutions are clearly observed at a constant flow rate of 17 ml/s as the tube cross-sectional area decreased due to increase in compressive transmural pressure. In addition, the viscosity of PAA is drastically decreased due to its high shear-thinning behavior than that of the CMC under same applied external pressure.

Introduction

The investigation of fluid flow characteristics in elastic inflatable and collapsible tubes is important to bio-fluid mechanics encountered in the human body and other applications; for instance, transport of food and liquids in human throat (pharynx), tube (esophagus) connecting the throat and stomach, and intestines; blood flow through the veins capillaries and arteries (Wyk et al., 2015; Cherry and Eaton, 2013); airflow in the pulmonary airways. The knowledge of the mechanisms of pharyngeal, esophageal and intestinal transport of food and liquids is very useful for the treatment of patients with the malfunctioning of these transport processes. The physiology of these applications in the human body is very complex and is not fully understood. Therefore, the presented research work is motivated to investigate in model experiments the flow behavior of Newtonian and non-Newtonian fluids in a collapsible elastic tube under the influence of expansive and compressive transmural (internal minus external) pressures using Starling Resistor.

1

Fluid flow in elastic tubes is a large displacement fluid-structure interaction problem encountered in biofluid mechanics (Meng et al., 2005), peristaltic pumping (Shapiro et al., 1969, Nahar et al., 2012b) and other applications. Several works on the study of flows in collapsible tubes and channels have been well documented based on the intended biological applications (Grotberg and Jensen, 2004; Kamm and Pedley, 1989; Pedley, 1980; Rana and Murthy, 2016; Shapiro, 1977a,b). Biofluid mechanics is important to the flow of fluids through vessels in the human body, as numerous fluid conveying vessels are elastic and subject to buckle non-axisymmetrically when the transmural pressure falls below a critical value (Heil, 1997). The interactions between the internal flow and wall deformation of these flexible elastic vessels determine the biological function or dysfunction. The examples of such vessels are the veins above the level of the heart, the airways during forced expiration, the pulmonary capillaries and the blood vessels in the heart muscle during systole (Conrad, 1969; Pedley, 1980). Holt (1941) investigated how the collapse of veins might affect peripheral venous pressure. He set up a model where water flowed through a rigid pipe to a collapsible segment of thin-walled rubber tubing and out through a more rigid pipe. The exact flow and wave propagation in distended tubes is well understood (Lighthill, 1975), whereas the flow structure in collapsed vessels is not fully understood. The problem of flow in collapsible tubes has been extensively studied experimentally by many authors (e.g. (Bertram et al., 1990; Conrad, 1969; Elad et al., 1992; Gavriely et al., 1989). The Starling Resistor is a classical bench-top experimental set up which is widely used (Grotberg and Jensen, 2004; Hazel and Heil, 2003; Heil, 1997; Holt, 1941; Katz et al., 1969; Knowlton and Starling, 1912; Lyon et al., 1980; Shapiro, 1977b) to investigate flow through elastic tubes relevant to many applications. This involves a pressure chamber that encloses a finite-length elastic tube mounted between two rigid tubes and fluid is pumped through the tube at a steady volume flow rate. The tube's large deformation during the buckling is found to lead to a strong interaction between the fluid and solid mechanics which is described by non-linear shell theory (Heil, 1997). Steady flow through a collapsible tube is found to be a multiple-valued function of the pressure drop across it, named as flow-controlled nonlinear resistance, (QNLR) (Conrad, 1969), where systematic experimental pressure-flow curves for both steady and unsteady flow conditions are presented. The significant system parameter for changes in tube cross-section is transmural pressure, which in turn affect the flow geometry. The typical fluid-structure interaction problem involving the flow passing a collapsible tube has been studied both experimentally and theoretically, and represented with a relationship between transmural pressure and cross-sectional area and the factors which influence it (Bertram, 1986, 1987; Elad et al., 1987; Flaherty et al., 1972; Jensen and Pedley, 1989; Katz et al., 1969; Scroggs et al., 2004; Shapiro, 1977b; Zhu and Wang, 2003, Neelamegam and Shankar, 2015, Raj et al. 2018, Amaouche and Labbio, 2016). On the other hand, Lyon et al. (1980) proposed the hypothesis for the pressure-flow relationships by the waterfall model studied in a Starling Resistor described, only for flows with lower Reynolds numbers. Whereas, the minimum Reynolds number for self-excited oscillation is precisely determined experimentally by Bertram and Tscherry (2006). There are few theoretical investigations of both the flow and the wall mechanics in three-dimensional collapsible tubes (Heil, 1997, 1998; Heil and Pedley, 1996; Marzo et al., 2005; Roser and Peskin, 2001, Anand et al. 2019). In addition, the wall deformation and fluid flow have been modeled using geometrically nonlinear shell theory and lubrication theory respectively (Heil and Pedley, 1996; Rosmery et al., 1977; Unhale et al., 2005; Whittaker et al., 2010). If the transmural pressure acting on the tube is sufficiently negative then the tube buckles non-axisymmetrically and the subsequent large deformations lead to a strong interaction between the fluid and solid mechanics (Hazel and Heil, 2003). The extensive experimental and theoretical contributions (Ghazy et al., 2018; Kozlovsky et al., 2014, Nahar et al., 2013) made by several authors mentioned above

are of great value for the scientific community as well in the many biomedical and biomechanical applications. These enable a better understanding of the laminar and turbulent flows of Newtonian fluids through collapsible tubes and the solid mechanics of the tube. In contrast, there is little literature (Dodson et al., 1974; Nahar et al., 2012a) on the experimental flow characteristics of non-Newtonian fluids through elastic tubes under the influence of different transmural pressures involving the interaction of the deformed tube wall with the fluids. In addition, there is also little information available on the unsteady-periodic flow or peristaltic-squeezing of elastic tubes for the transport of such fluids. This investigation is important as the determination of time scales involved in the transport of non-Newtonian fluids is relevant to the transport of food in the human gastrointestinal tract and other applications. The investigation methods for the shape of the deformed elastic tube and the corresponding flow field are also not yet well established. The local tube cross-sectional area has been measured by an electrical impedance technique (Kececioglu et al., 1981) or ultrasound imaging (Bertram and Ribreau, 1989) or remote sensing technique (Elad et al., 1989). The cross-section is assumed to remain the same throughout the tube as the same amount of liquid is flowing with same mean velocity through each cross-section at any given time (Holt, 1959). In contrast, different cross-section of vessel or rubber tube showing changes in shape during oscillations of pressure is also observed (Brooks and Luckhardt, 1916). Kresch and Noordergraaf (1972) has proposed a mathematical analysis for the cross-sectional shape of a flexible tube as its internal pressure varies. Quantitative results are presented in terms of the physical parameters of the tube, such as wall thickness and Young's modulus. In the present study, the different degree of deformed tube shapes are aimed to quantify by means of computer tomography method where a grid line pattern is constructed on the tube surface and several images are taken at different angles around the tube radius.

Experiment

The study of flow behavior in a collapsible elastic tube includes the investigation of the fluid-structure interaction involving the flow passing through it (Zhu and Wang, 2003). There is very few published literature (Dodson et al., 1974; Nahar et al., 2012a) on the experimental flow characteristics of non-Newtonian fluids in collapsed elastic tubes under the influence of compressive external pressures. Therefore, aqueous solutions of one Newtonian and two non-Newtonian shear-thinning fluids have been used. The solutions have been characterized by rheological measurements. The collapsed elastic tube shapes (under the influence of transmural pressures) are determined using computer tomography (CT) based image analysis and the corresponding fluid flow velocity profiles are monitored by UVP technique. These CT and UVP methods are described in detail elsewhere (Nahar et al., 2012a).

PEG aqueous solution as a Newtonian fluid

Polyethylene Glycol (PEG, MW $\approx 3.5 \times 10^4$ g/mol; Clariant, Switzerland) aqueous solution (19.67 % w/w) is used as a Newtonian fluid to investigate the steady flow behavior through collapsible elastic tubes. The solution is prepared using a rotor-stator device (Polytron PT6000, Kinematica AG) at a constant temperature, T = 22 ºC.

CMC and PAA aqueous solutions as non-Newtonian fluids

Carboxymethyl-cellulose (CMC; Blanose CMC 7MF, IMCD Switzerland AG) at 1.5 % w/w (with 0.1 M NaCl; MW = 2.5×10^5 g/mol) and Polyacrylamide (PAA; SNF FLOERGER, France) at 0.01 % w/w (MW $\approx 14 \times 10^6$ g/mol) aqueous solutions are used as non-Newtonian

shear-thinning fluids. CMC and PAA aqueous solutions are found to be less and highly shear-thinning respectively with about the same value of zero shear viscosity. All those aqueous solutions are again prepared using a rotor-stator device at T = 22 °C.

Elastic tube

A silicone elastic tube (Lindemann GmbH, Germany) with 20 mm inner diameter and 1 mm thickness is used in the model flow experiments. The elastic modulus of the tube is measured by the stress-strain curve using Zwick device (Zwick Roell Z010, Zwick GmbH, Germany). It was seen that the elastic modulus (stress to strain ratio) of the tube decreased with increase in strain. Since tube deformation in the present study is expected to be low, therefore, the elastic modulus of the tube (E = 4.7MPa) was taken by linear fit of the stress-strain curve at the lower deformation region.

Starling Resistor

Several authors e.g. (Lyon et al., 1980) used the Starling Resistor setup for Newtonian fluid flow investigations in elastic tubes relevant to many applications. Figure-1 shows the present experimental setup consisting of a 300 mm inner diameter, 5.66 mm thick and 620 mm long cylindrical plexiglass (PG) pressure chamber fixed on each side a metal flange with an aluminum pipe. A silicone elastic tube (320 mm in length, 20 mm inner diameter, 1 mm thickness), is mounted between the two aluminum pipes with a slight axial extension to avoid the longitudinal bending especially when the tube inflates. The different states of the tube geometry are achieved by increasing the hydrostatic head connected with the water-filled PG pressure chamber. The aluminum pipe on the right side is connected to a gear pump (MCP-Z, ISMATEC) and a PVC tank, which contains the investigated fluids for flow through the collapsible elastic tube. All the consequent measurements are carried out at 22 °C in this study.
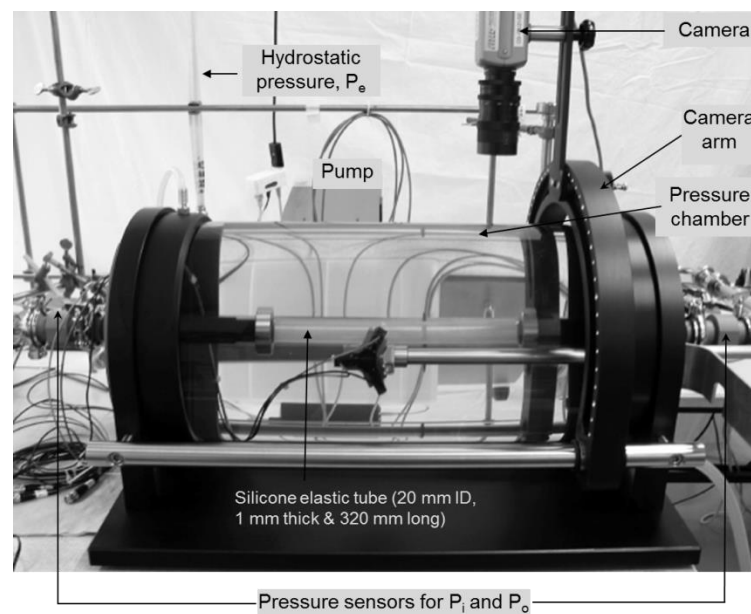

Figure-1: Experimental set up for flow behavior study of different fluids (Newtonian and non-Newtonian) through a collapsible elastic tube using Starling Resistor.

Results and Discussion

Rheology of fluids

The rheological properties such as shear rate dependent viscosities and frequency-dependent dynamic storage and loss moduli are measured using an Anton Paar Physica (MCR 300) rheometer with concentric cylinder geometry (CC27, shear gap width = 1.13 mm) to confirm the concentration for similar zero shear viscosity and the corresponding inelastic behavior of the investigated fluids. The rheological measurements are carried out at T = 22 ºC, which is also maintained in the flow loop used during the experiment.

Shear rate dependent viscosity

The measured shear rate dependent viscosities of the investigated fluids (PEG, CMC and PAA aqueous solutions at 19.67, 1.5 and 0.01 % w/w respectively) showed about the similar value of shear viscosity ($\eta_0 \approx 0.143$ Pa.s) at the shear rate of 0.11/s as in Figure-2. Both non-Newtonian (1.5 % CMC and 0.01 % PAA) aqueous solutions represented the shear thinning behavior, while one being highly shear-thinning (0.01 % PAA) than the other (1.5 % CMC) at the same applied shear rate ranges. No significant variation in the solution properties and the temperature is observed while passing through the flow loop used in the experiment (the duration was $\approx$ 30min to 1h). The shear rate dependent viscosity of the investigated solution is measured again after performing the flow experiment and no change in the flow curve is attained.
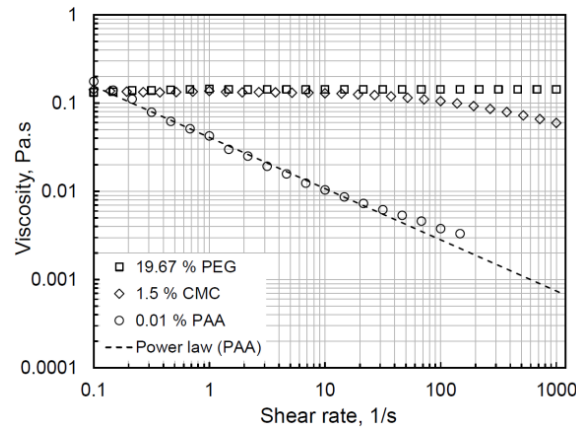

Figure-2: Measured shear rate dependent viscosities of aqueous fluids of PEG (19.67%), CMC (1.5%) and PAA (0.01%) representing the similar value of shear viscosity at a shear rate of 0.01s^{-1}.

Inelastic behavior of the shear-thinning fluids

The two shear-thinning aqueous solutions (1.5 % CMC and 0.01 % PAA) are further investigated to measure the viscous modulus, G'' and elastic modulus, G' under linear viscoelastic conditions of the oscillatory shear. G'' is seen to be an order of magnitude higher than G' for 1.5 % CMC (Figure-3a). Whereas 0.01 % PAA (Figure-3b) shows a slightly higher value of G" than G', indicating their inelastic shear thinning behavior. In contrast, the aqueous solution of 2.5 % CMC depicts dominating elastic properties with increasing frequency (Figure-3a), which is typical viscoelastic behavior. The inelastic shear-thinning

fluids are chosen in the present study to avoid the complex behavior under imposed flow conditions.
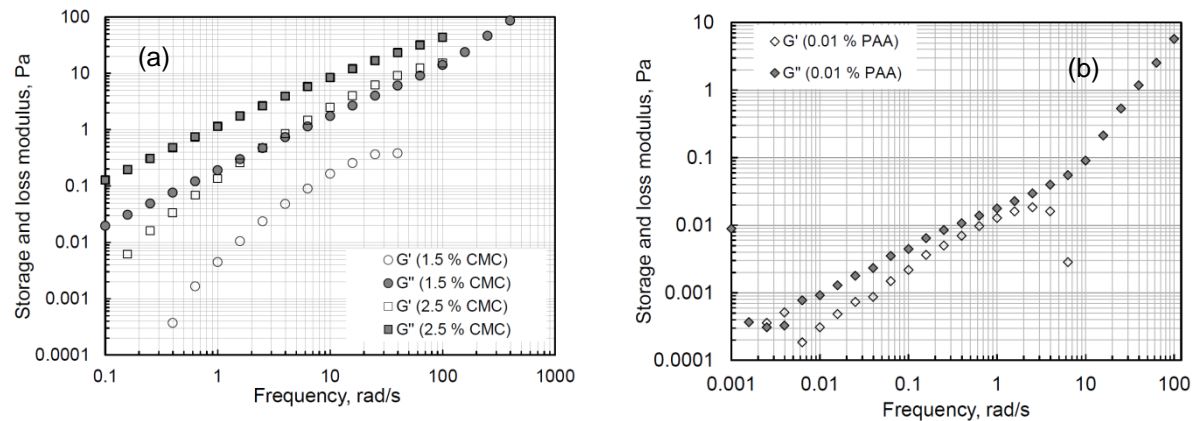

Figure-3: Frequency dependent elastic (G') and loss (G") moduli using oscillatory shear measurements with a constant deformation of 5 % at 22 °C for (a) CMC and (b) PAA aqueous solutions.

Tube shapes under various Transmural pressures (P_{tm}) at a constant flow rate ($\dot{Q}$)

Experimentally adjusted hydrostatic head connected with the water-filled PG pressure chamber (as in Figure-1) resulted to various states of the tube shapes; uncollapsed (at P_e = 18 mbar or $P_{tm(down)}$ = 79 mbar) and collapsed (at P_e = 105 mbar or $P_{tm(down)}$ = - 18 mbar), while flowing of Newtonian (PEG) and non-Newtonian (CMC & PAA) aqueous solution through it. The investigated length for tube shape (both uncollapsed & collapsed) is chosen to be 190 mm from the rigid tube connection from the outlet. The collapsed tube shape is representing the region of strongest collapse near the downstream end as the fluid pressure decreases continuously in the stream-wise direction leading to a higher compression of the tube wall. Figure-4 represents the influence of flowing fluid properties on the variation in deformation along the tube length under different applied external pressures. The boundary lines around the tube are drawn for clear visualization of tube deformation depending on the fluid flowing through it. The elastic tube is seen to be less collapsed for the Newtonian (19.67 % PEG) fluid, whereas it is more collapsed for inelastic shear-thinning fluids (1.5 % CMC and 0.01 % PAA) exhibiting the same shear viscosity at a shear rate of 0.1 s^{-1} and under same imposed external pressures. The reason is that the internal pressure is minimized by increasing the fluid velocity during tube collapse by external pressure for the shear-thinning fluids.

Figure-5 shows the variation in tube geometry and the corresponding velocity profiles at constant length (X = 7 cm from the rigid tube connection at the outlet) and $\dot{Q}$ = 17 ml/s under various downstream transmural pressures $P_{tm(down)}$. The inserted tube geometries were analyzed under different applied P_e while a steady flow of 1.5 % CMC aqueous solution through the tube. The detail description of tube shape analysis (CT-method) and flow profile measurement (UVP) are given elsewhere (Nahar et al., 2012a). The tube geometries were also assumed to attain the same shapes with slight variation in the cross-sectional area during steady flow of 19.67 % PEG or 0.01 % PAA solution in the tube. It can be seen that the tube shape changed from circular to two-lobed shape, and the corresponding velocity profiles

transformed from parabolic to bimodal for both Newtonian and non-Newtonian fluids. The elastic tube exhibited a circular shape for positive $P_{tm(down)}$ with a parabolic velocity profile, where the more shear-thinning fluid (0.01 % PAA) showed flattened profile at the tube center as expected. The $P_{tm(down)}$ was found to be more positive for Newtonian fluid than that of the shear-thinning fluids, since the internal pressure P_o was much higher than the applied external pressure P_e. As long as the $P_{tm(down)}$ became sufficiently negative, the elastic tube started to buckle from an elliptical to a two-lobed shape.

A reduction in the tube cross-sectional area can lead to an increase in both the near-wall and average shear rates during a steady flow of both Newtonian and shear-thinning fluids. The average shear rate can be calculated using the obtained average velocity ($\dot{Q}/A$) in the tube where the cross-sectional area A was estimated by the image analysis. Since the maximum shear rate was estimated near the tube wall, therefore it was calculated with the corresponding velocity gradient at that regime. The approximated average and near-wall shear rates in the deformed elastic tube with the different cross-sectional area during flow of Newtonian and non-Newtonian fluids are summarized in Table-1.
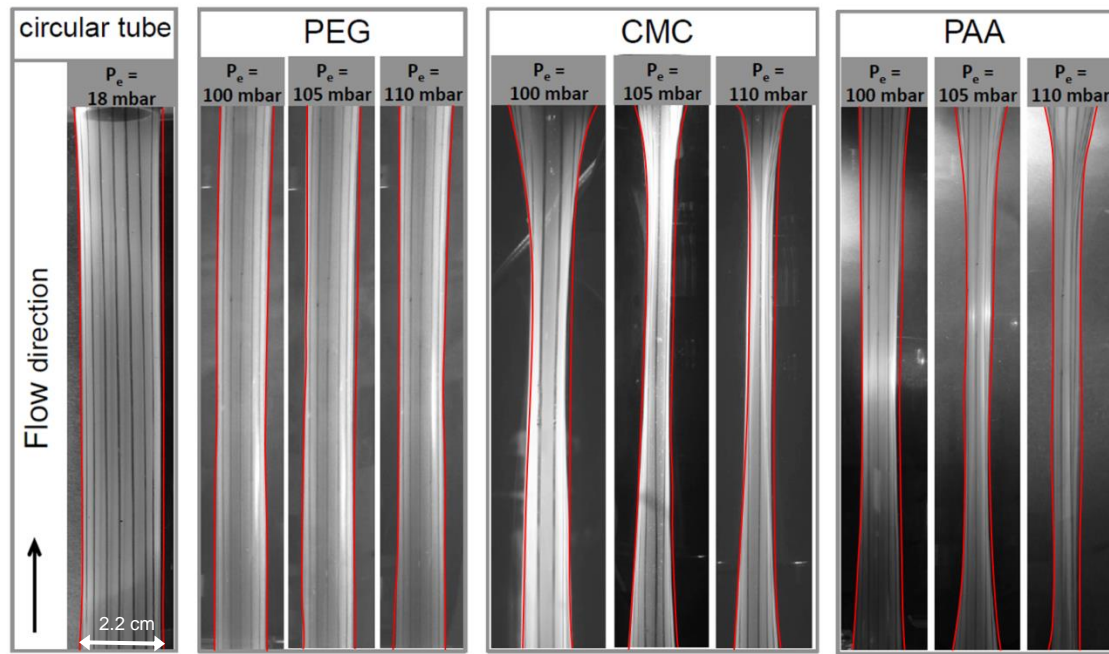

Figure-4: Influence of flowing fluid properties through the tube (with an inner diameter of 2.0 cm in the circular case and the wall thickness of 1.0 mm) on the variation in deformation along the tube length (front view) under different applied external pressures at $\dot{Q}=$ 17 ml/s.
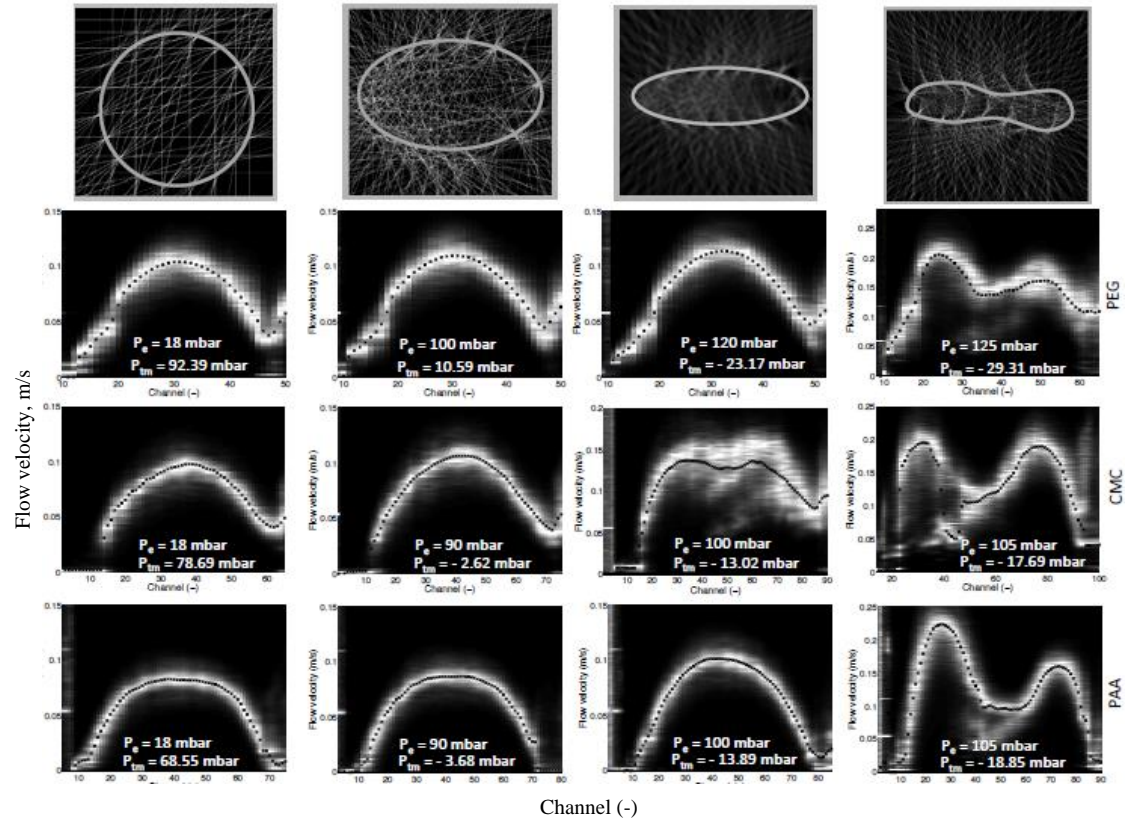
Figure-5: Influence of various applied transmural pressures on the change in tube shapes and the corresponding velocity profiles in the tube during a steady volume flow rate ($\dot{Q}$ = 17 ml/s) of PEG, CMC and PAA aqueous solutions.

Table-1: Comparison of the experimental and theoretical values of rheological properties for the investigated fluids (PEG, CMC, PAA) under different geometries of the collapsed elastic tube and applied pressures P_e. v_{avg} is the average velocity in the tube, and r_{eq} and Re are the equivalent radius and Reynolds number respectively. $\gamma_{0,avg}$ and η_{0avg} are the average shear rate and viscosity in the tube respectively, $\gamma_{0,local}$ and η_{0local} are the average shear rate and viscosity near the tube wall respectively.

	Applied P_e mbar	A mm^2 (CT method)	v_{avg} m/s	r_{eq} m	$\gamma_{0,avg}$ s^{-1}	η_{0avg} Pa.s	Re	$\gamma_{0,wall}$ s^{-1}	η_{wall} Pa.s
PEG	18	342	0.049	0.0104	19.03	0.143	7.25	10.52	0.143
	90	329	0.051	0.0102	20.13	0.143	7.38	-	-
	100	326	0.052	0.0100	20.42	0.143	7.42	-	-
	105	266	0.063	0.0092	27.64	0.143	8.74	25.5	0.143
	110	235	0.072	0.0086	33.35	0.143	8.21	-	-
CMC	18	342	0.050	0.0104	12.49	0.135	7.7	10.66	0.143
	90	285	0.059	0.0095	16.45	0.134	8.5	-	-
	100	114	0.149	0.0060	64.73	0.116	15.5	-	-
	105	52	0.327	0.0040	211.11	0.089	29.6	35.8	0.134
	110	32	0.538	0.0032	445.25	0.075	45.3	-	-
PAA	18	342	0.049	0.0104	11.69	0.0098	106	13.92	0.0095
	90	247	0.069	0.0088	19.06	0.0074	165	-	-
	100	82	0.21	0.0051	99.81	0.0028	748	-	-
	105	49	0.34	0.0039	211.75	0.0018	1487	57.4	0.0041
	110	22	0.77	0.0026	718.45	0.0009	4540	-	-

Effect of external pressure on variation in pressure drop with volume flow rate

The flow behavior of fluids in elastic tubes depends on the micro-structural properties of the fluids, solid mechanics of the tube, and the interaction between the deformation of the tube and fluids. The applied external pressure P_e should exceed a critical value to approach the different geometry of the tube shape (elliptical to line or area contacted two lobes). Figure-6a, 6b, 6c are representing the pressure drop in the tube ($\Delta P = P_i - P_o$) as a function of P_e and $\dot{Q}$ during a steady flow of the investigated fluids (PEG, CMC, PAA). It is seen that while flowing of Newtonian fluid (19.67 % PEG), ΔP at a given $\dot{Q}$ does not change until it reaches a critical P_e when the transition of partial to complete tube collapse occurs with reduced tube cross-sectional area. The applied critical P_e region is about 105 to 120 mbar as seen in Figure-6a. The three distinct regions of applied critical P_e for the tube deformation are also clearly observed. The value of critical P_e depends on the balance of the fluid normal $F_N(P)$ and tube wall compression F_{tube} forces with the applied external force $F_e(P_e)$, where the forces are almost at the equilibrium ($F_N + F_{tube} \cong F_e(P_e)$). It also shows that ΔP in the tube increases linearly with an increase in $\dot{Q}$ (schematic deformed tube shapes at $P_e = 120$ mbar for different $\dot{Q}$ and also at constant $\dot{Q} = 17$ ml/s for various applied P_e are also given) below the critical P_e region due to higher frictional force, as $\dot{Q}$ is a function of R_e rather than reduction in tube cross-sectional area A. On the other hand, ΔP is higher for lower $\dot{Q}$ at higher P_e since the tube cross-sectional area is reduced above the critical P_e region. Moreover, reduction in A is much higher at lower $\dot{Q}$ than that of the higher $\dot{Q}$ ($F_{Nhigher\,\dot{Q}} \geq F_{Nlower\,\dot{Q}}$) for a given P_e. Therefore, ΔP increases with increasing $\dot{Q}$ below critical P_e, and decreases above critical P_e until a given $\dot{Q}$ when the elastic tube is reopened to its original shape. The region of applied critical P_e (about 97 to 105 mbar) is again clearly observed in Figure-6b, 6c, where the transition of partial to complete tube collapse occurs, during steady flow of 1.5 % CMC and 0.01 % PAA solutions respectively. The same feature is also observed for various values of $\dot{Q}$ and the transition region for tube collapse is also found to be common for the range of $\dot{Q}$ used in the present work. It is also seen that ΔP in the tube increases slightly linearly with increase in P_e at a constant $\dot{Q}$ below the critical P_e region. In contrast, above the critical P_e region, ΔP increased drastically involving a small non-linearity for the same $\dot{Q}$ since the tube walls come closer reducing A at higher P_e and increased the fluid friction on the tube wall. In addition, the slope in the upper critical P_e region is found to be about 48 times higher than that at the lower critical P_e region. Since ΔP in a pipe is a nonlinear function of the cross-sectional area (according to Darcy-Weisbach equation: $\Delta P = fL\rho v^2/2D$ (Green and Perry, 2008), where f is the friction factor, $D = \sqrt{4A/\pi}$ is the diameter of tube of length L and v is the average velocity of fluid of density ρ), the nonlinearity present in the upper critical P_e region can, therefore, be due to reduction in tube A. Figure-6b shows that $\Delta P(= P_i - P_o)$ increases with increase in $\dot{Q}$ of CMC aqueous solution up to critical P_e due to increasing of velocity and corresponding friction force in uncollapsed tube. When the applied P_e is further increased from the critical value so that the transmural pressure difference becomes more negative, then the collapsed tube walls come closer reducing in A and ΔP is increased at a given $\dot{Q}$. On the other hand, as $\dot{Q}$ is further increased, internal pressure is gradually increased and the tube recovered its original shape at higher $\dot{Q}$ thereby decreasing ΔP due to increase of A and decreasing the corresponding average flow velocity in the tube. The situation is better explained by the observation of the tube geometry at the highest applied P_e in this experiment (the change in the observed tube shape at the corresponding flow rate is schematically drawn in Figure-6). It is seen that an area contacted collapsed tube shape is formed in the lower $\dot{Q}$ range with reduced A. As $\dot{Q}$ is slowly increased, the tube

opens up and increasing its A (due to deformability caused by tube elasticity), which results in a decrease of ΔP in the tube.
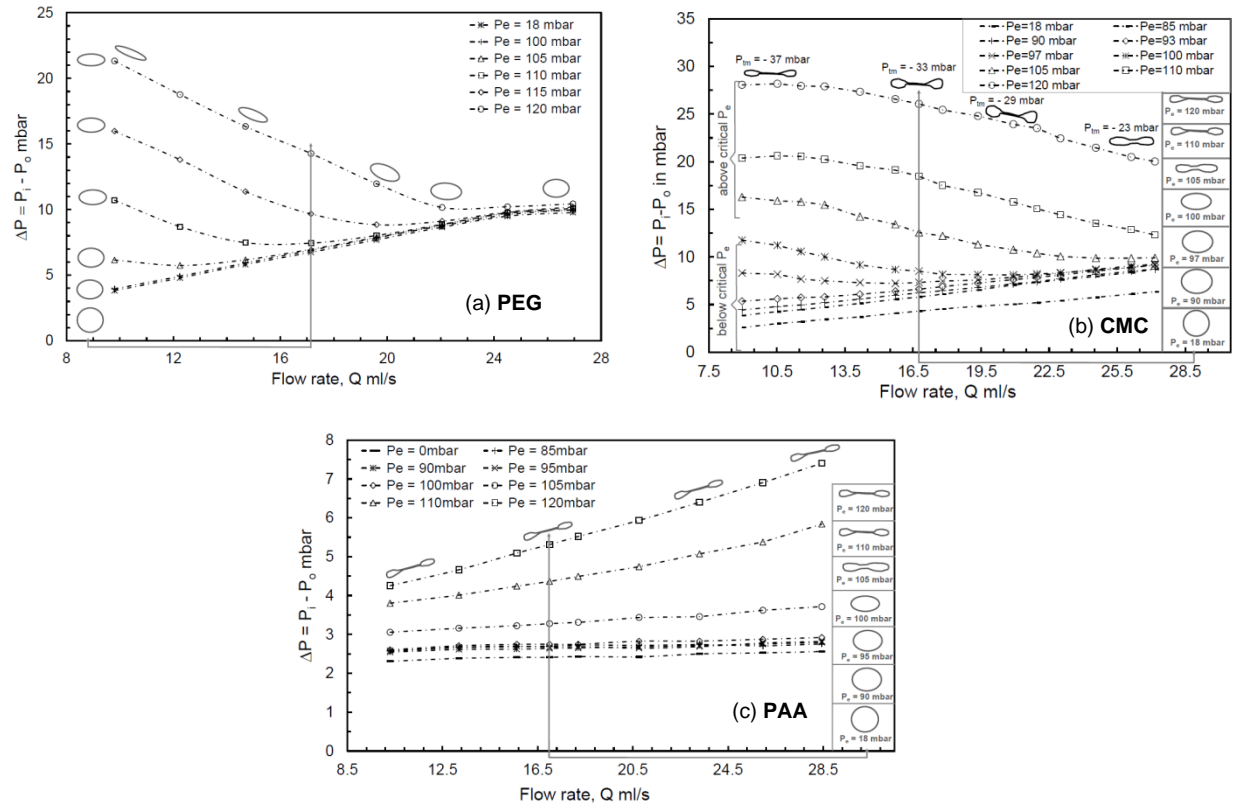

Figure-6: Influence of applied external chamber pressure on the variation in pressure drop with a steady volume flow of (a) Newtonian (PEG) and (b) (c) non-Newtonian (CMC, PAA) aqueous solution in the elastic tube together with its schematic deformed shapes at constant $\dot{Q}$ = 17 ml/s for various applied P_e.

On the other hand, for high shear-thinning fluid (PAA) the critical Pe is found to be closer to each other for all $\dot{Q}$ compared to the other investigated fluids as in Figure-6c. The reason is that, $\dot{Q}$ does not have much influence on the increase in tube internal pressure rather than a reduction in A, which can be observed above the critical P_e. In addition, the investigated range of $\dot{Q}$ is not to be high enough to increase the tube internal pressure due to increase in the fluid velocity (high shear thinning). Therefore, the shape of the tube at a given P_e does not change while increasing $\dot{Q}$, and correspondingly ΔP is increased for higher $\dot{Q}$ due to increase in frictional force inside the tube as shown in Figure-6. It is also seen that ΔP is much higher for the deformed tube due to much higher reduction in A compared to the other investigated fluids (PEG and CMC).

Effect of collapsed elastic tube geometry and velocity profile on fluid rheological properties

Figures-7a, 7b, 7c show the qualitative summary of the flow characteristics of the investigated fluids (Newtonian and non-Newtonian) through a deformed elastic tube. The variation in average flow velocity, the shear rate, and the viscosity are represented as a function of tube cross-sectional area, where all the quantities are defined as dimensionless. The reference average flow velocity ($v_0 = \dot{Q}/A_0$) in the undeformed tube used is about 0.05

m/s at $\dot{Q}$ = 17 ml/s for PEG, CMC and PAA aqueous solutions. It can be seen that the velocity ratio ($\beta = v/v_0$) increases by an order of magnitude fitting with a power law ($\beta = 1.0005\alpha^{-1}$) for a decrease in area ratio by less than a factor of two during steady flow of PEG aqueous solution. The average shear rate γ_0 for $\dot{Q}$ = 17 ml/s in the undeformed tube is estimated by $\gamma_0 = 4\ v_0/r_0 = 21 s^{-1}$ for Newtonian fluid. The equivalent radius r_{eq} (= $\sqrt[2]{A}/\pi$) is calculated from the experimentally obtained tube cross-sectional area A by tube shape analysis (described elsewhere by Nahar et al., 2012). It is found that the shear rate ratio ($\dot{\Gamma} = \dot{\gamma}/\dot{\gamma}_0$) in the deformed tube increased only by a factor of two, which is again fitted well by a power law as $\dot{\Gamma} = 1.0008\ \alpha^{-1.5}$ and the corresponding average viscosity in the tube is found to be constant for PEG. All the calculated relevant flow parameters for PEG are summarized in Table-1. On the other hand, β also increases by an order of magnitude for moderate shear-thinning fluid (CMC) fitting with a power law ($\beta = 1.0109\ \alpha^{-1.0037}$) where the area ratio decreases by more than an order of magnitude. Here, the average shear rate γ_0 for $\dot{Q}$ = 17 ml/s in the undeformed tube is estimated by $\dot{\gamma}_0 = \int_0^{req} \dot{\gamma} r dr = \int_0^{req} r dr = (2v_0/r_{eq})(3n+1)/(2n+1) = 14 s^{-1}$ assuming a non-Newtonian shear thinning power-law liquid. The power-law index n is 0.8208 for CMC solution and the corresponding average viscosity in the tube is calculated using the Carreau equation. It is found that the shear rate ratio ($\dot{\Gamma}$) in the deformed tube increased by a factor of 50, which is again fitted well by a power law $\dot{\Gamma} = 1.0156\ \alpha^{-1.5056}$. The corresponding viscosity ratio ($\Lambda = \eta/\eta_0$) decreased by a factor of two is fitted by $\Lambda = \Lambda_0 + k_1(1 - e^{-k_2\alpha})$ where the fitted constants are $\Lambda_0 = 0.1407$, $k_1 = 0.85$ and $k_2 = 6.243$. $\Lambda_0 = \eta_m/\eta_0 = 0.1407$ is the minimum viscosity ratio, where $\eta_m = 0.0193$ Pa.s is the average minimum viscosity when the tube cross-sectional area $A \to 0$, and 0 = 0.137 Pa.s is the average viscosity in the undeformed tube. In addition, β is also seen to be increased by an order of magnitude for high shear-thinning fluid (PAA) fitting with a power law ($\beta = 1.0005\alpha^{-1}$) for a decrease in area ratio also by more than an order of magnitude. The average shear rate $\dot{\gamma}_0$ in the undeformed tube is 13 s^{-1} (assuming non-Newtonian shear-thinning power-law liquid). The power-law index n is 0.42 for high shear thinning PAA solution and the corresponding average viscosity in the tube is obtained using the Carreau equation. The shear rate ratio ($\dot{\Gamma}$) in the deformed tube increased by more than a factor of 90, which is again fitted well by a power law $\dot{\Gamma} = 1.0022\alpha^{-1.5}$. The corresponding viscosity ratio (Λ) decreased by a factor of fourteen is fitted by $\Lambda = 0.9996\alpha^{0.87}$. Here the $\eta_m = 0.00038$ Pa.s (the average minimum viscosity when the tube cross-sectional area $A \to 0$) is approximated by a linear fit ($\Lambda = \Lambda_0 + k\alpha$, with $\Lambda_0 = 0.0414$ and $k = 0.9625$). The viscosities of CMC and PAA solutions are found to decrease while flowing at $\dot{Q}$ = 17 ml/s through an elastic tube under different compressive P_{tm}, the values of which are well comparable with the off-line rheological measurement (Table-1). As P_e increases from 18 to 105 mbar, the average shear rate near the tube wall increases from 10.66 to 35.8 s^{-1} with the corresponding viscosity of 0.143 to 0.134 Pa.s (for CMC). Whereas the average wall shear rate also increases from 13.92 to 57.4 s^{-1} for PAA with a decrease in shear-thinning regime. The viscosity of PAA is drastically decreased due to its high shear-thinning behavior than that of the CMC under same applied P_e. At low P_e = 18 mbar, the average shear rates in the tube and near the wall are found to be same value of about 11 s^{-1} and 13 s^{-1} for CMC and PAA respectively. At high P_e = 105 mbar, the average shear rate in the tube becomes almost equal to the average shear rate near tube wall thereby causing the fluid shear-thinning over whole of the tube cross-section for both shear-thinning fluids. The decrease in the viscosity of a non-Newtonian fluid is useful to enhance the nutrient transport through the small intestine during digestion. The calculated Reynolds number Re (= $2\rho v_{avg}\ r_{eq}/\eta_{avg}$, as listed in Table-1, Table-2, Table-3) increased by a factor of seven for CMC in deformed tube (Re = 55.8 at P_{tm} = - 30 mbar) compared to that in the undeformed tube (Re = 7.7), which confirms the flow region as laminar in the collapsible

elastic tube. Whereas, for PAA the calculated Re increased by a factor of sixty in deformed tube ($Re = 6729$ at $P_{tm} = -30$ mbar) compared to that in the undeformed tube ($Re = 105$), which indicates that the flow is transforming to the turbulent regime due to high increase in the velocity for shear-thinning fluid.
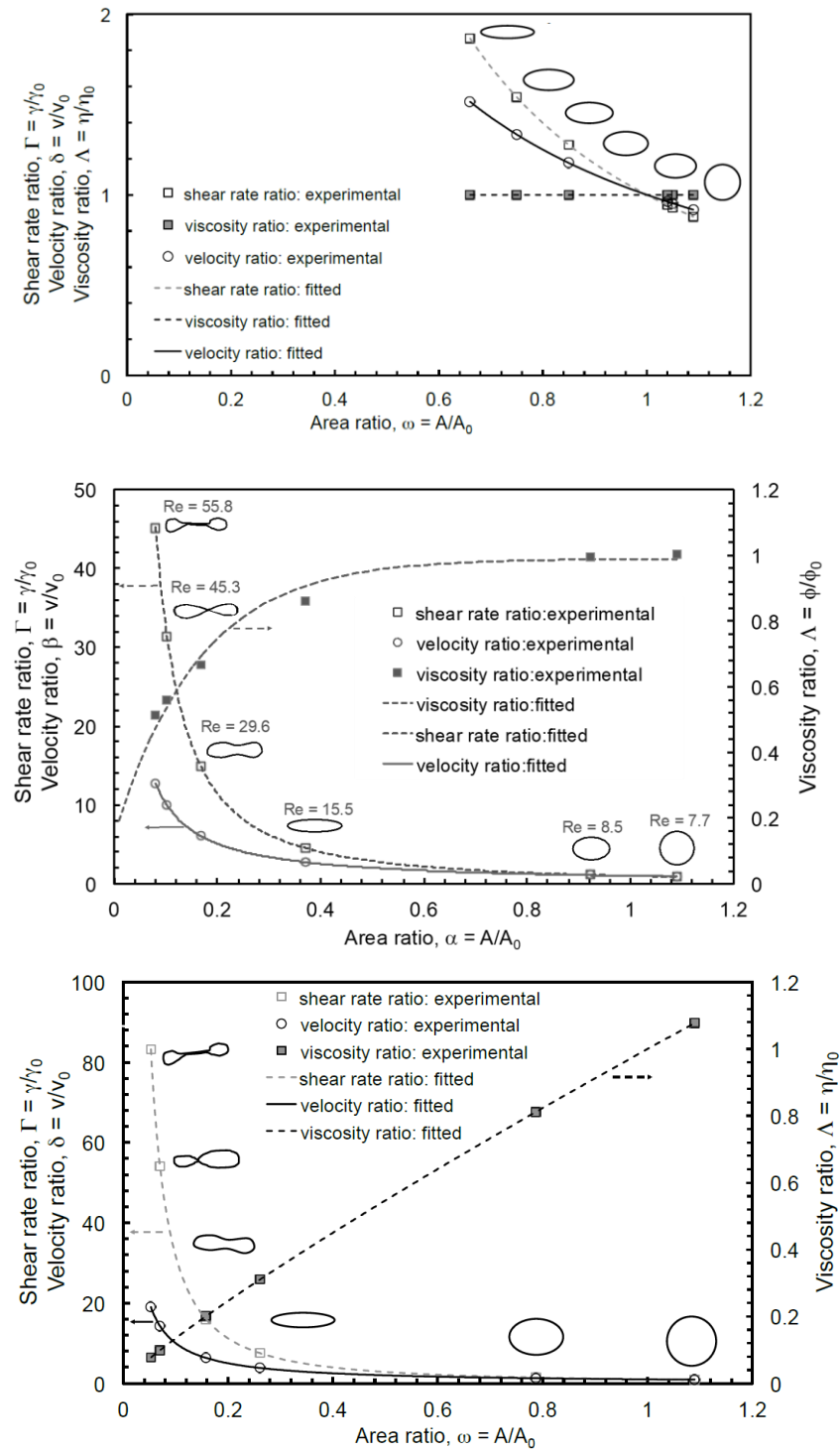

Figure-7: Fluid flow characteristics of (Top) Newtonian (PEG), (middle) non-Newtonian (CMC), and (bottom) non-Newtonian (PAA) aqueous solution during steady flow through a deformed elastic tube.

Conclusion

The steady flow characteristics of both Newtonian and non-Newtonian shear-thinning fluids through a collapsible elastic tube are investigated under different compressive transmural pressures in a Starling Resistor setup. The present study shows the influence of inelastic fluid behavior, elastic tube and fluid interaction on the fluid flow characteristics, the effect of external pressure on variation in pressure difference and elastic tube deformation. At a certain applied external pressure, the deformation of an elastic tube depends not only on its modulus but also on the fluids flowing through it. It is found that higher tube deformation resulted for higher shear-thinning fluid, as the outlet pressure in collapsed tube is lower due to reduced cross-sectional area and the corresponding compressive downstream transmural pressure is more negative than that at the upstream. The tube cross-sectional area decreased by only about factor of one for PEG and about factor of six for both CMC and PAA from the undeformed one under an applied P_e of 105 mbar. The corresponding maximum velocity increased by a factor of two during steady flow of shear-thinning fluids. Furthermore, the cross-sectional area decreased by an order of magnitude from the undeformed one when $P_{tm(down)}$ is about -30 mbar for both shear-thinning fluids due to increase in compressive transmural pressure. However, the viscosity of PAA is drastically decreased due to its high shear-thinning behavior than that of the CMC under same applied P_e. Therefore, the high shear-thinning fluids can be considered for efficient nutrient transport through the small intestinal wall during digestion. In addition, the steady flow of a non-Newtonian fluid through a collapsed elastic tube is simulated and compared with the corresponding experimental data reported elsewhere (Tanner et al., 2012). A good agreement between simulation and experiment is obtained with additional insight by considering the local quantities for shear rates and viscosities.

Acknowledgments

Notation

Symbol	Unit	Meaning
A	m^2	cross-sectional area of deformed tube
A_0	m^2	cross-sectional area of undeformed tube
D	m	elastic tube diameter
E	MPa	elastic modulus of the tube
f	-	friction factor
F_e	N	applied external force
F_N	N	fluid normal force
F_{tube}	N	tube wall compression force
g	ms^{-2}	gravity constant
G'	Pa	storage modulus
G''	Pa	loss modulus
k_1, k_2	-	fitting constant
l, L	m	length of the tube
n	-	power-law index
P_e	mbar	external chamber pressure
P_i	mbar	inlet pressure
P_o	mbar	outlet pressure
P_{tm}	mbar	transmural pressure difference
$P_{tm(down)}$	mbar	downstream transmural pressure
$P_{tm(up)}$	mbar	upstream transmural pressure
$\dot{Q}$	ml s^{-1}	volume flow rate
r_0	m	internal radius of undeformed tube
Re	-	Reynolds number
r_{eq}	m	equivalent radius of deformed tube
v_0	ms^{-1}	reference average flow velocity
v_{avg}	ms^{-1}	average fluid velocity in the undeformed tube
α, ω	-	cross sectional area ratio (A/A_0)
β	-	velocity ratio (v/v_0)
$\dot{\gamma}$	s^{-1}	average shear rate in the deformed tube
$\dot{\gamma}_0$	s^{-1}	average shear rate in the undeformed tube
$\dot{\gamma}_{avg}$	s^{-1}	average shear rate in the deformed tube
$\dot{\gamma}_{wall}$	s^{-1}	average shear rate near the tube wall
$\dot{\Gamma}$	-	shear rate ratio ($\dot{\gamma}/\dot{\gamma}_0$)
ΔP	mbar	pressure difference
η	Pa.s	shear viscosity of the fluid
η_0	Pa.s	zero shear viscosity
η_{avg}	Pa.s	average viscosity in the deformed tube
η_{wall}	Pa.s	average viscosity near the tube wall
η_m	Pa.s	average minimum viscosity when $A \rightarrow 0$
Λ	-	viscosity ratio (η/η_0)
Λ_0	-	minimum viscosity ratio (η_m/η_0)
π	-	Pi-number
ρ	kg m^{-3}	density

Abbreviations

Symbol	Definition
CMC	Carboxymethyl Cellulose
CT	Computer Tomography
PAA	Polyacrylamide
PEG	Polyethylene Glycol
PG	Plexiglass
UVP	Ultrasound Velocity Profiling

References

Amaouche, M. and Labbio, G. D. Linear and weakly nonlinear global instability of a fluid flow through a collapsible channel. Physics of Fluids 28, 044106, 2016.

Anand, V., David, J. and Christov, I. C. Non-Newtonian fluid-structure interactions: Static response of a microchannel due to internal flow of a power-law fluid. Journal of Non-Newtonian Fluid Mechanics, 264:62-72, 2019.

Bertram, C. D. Unstable Equilibrium Behaviour in Collapsible Tubes. Journal of Biomechanics, 19:61-69, 1986.

Bertram, C. D. The Effects of Wall Thickness, Axial Strain and End Proximity on the Pressure-Area Relation of Collapsible Tubes. Journal of Biomechanics, 20:863-876, 1987.

Bertram, C. D., Raymond, C. J., and Pedley, T. J. Mapping of instabilities during flow through collapsed tubes of differing length. Journal of Fluids and Structures, 4:125-153, 1990.

Bertram, C. D. and Ribreau, C. Cross-sectional area measurement in collapsed tubes using the transformer principle. Medical and Biological Engineering and Computing, 27:357–364, 1989.

Brooks, C. and Luckhardt, A. B. The Chief Physical Mechanisms Concerned in Clinical Methods of Measuring Blood Pressure. American Journal of Physiology, 40:49-74, 1916.

Cherry, E. M., and Eaton, J. K. Shear-thinning effects on blood flow in straight and curved tubes, Physics of Fluids 25, 073104, 2013.

Conrad, W. A. Pressure-Flow Relationships in Collapsible Tubes. IEEE Transactions on Biomedical Engineering, 16:284-295, 1969.

Dodson, A. G., Townsend, P., and Walters, K. Non-Newtonian Flow in Pipes of non-Circular Cross Section. Computers and Fluids, 2:317-338, 1974.

Elad, D., Roger, D. K., and Shapiro, A. H. Choking Phenomena in a Lung Like Model. Transactions of the ASME Journal of Biomechanical Engineering, 109:19, 1987.

Elad, D., Sahar, M., Avidor, J. M., and Einav, S. Steady Flow Through Collapsible Tubes: Measurements of Flow and Geometry. Transactions of the ASME Journal of Biomechanical Engineering, 114:84-91, 1992.

Elad, D., Sahar, M., Einav, S., Avidor, J. M., Zelster, R., and Rosenberg, N. A novel non-contact technique for measuring complex surface shapes under dynamic conditions. Journal of Physics E: Scientific Instruments, 22:279-282, 1989.

Flaherty, J. E., Keller, J. B., and Rubinow, S. I. Post Buckling Behavior of Elastic Tubes and Rings with Opposite Sides in Contact. SIAM Journal on Applied Mathematics, 23:446-455, 1972.

Gavriely, N., Shee, T. R., Cuggel, D. W., and Grotberg, J. B. Flutter inflow limited collapsible tubes: a mechanism for generation of wheezes. Journal of Applied Physiology, 66:2251-2261, 1989.

Ghazy, M., Elgindi, M. B. and Wei, D. Analytical and numerical investigations of the collapse of blood vessels with nonlinear wall material embedded in nonlinear soft tissues. Alexandria Engineering Journal, 57(4): 3437-3450, 2018.

Green, D. W. and Perry, R. H. Perry's Chemical Engineers' Handbook. McGraw-Hill, New York, 2008.

Grotberg, J. B. and Jensen, O. E. Biofluid Mechanics in Flexible Tubes. Annual Review of Fluid Mechanics, 36:121-147, 2004.

Hazel, A. L. and Heil, M. Steady finite-Reynolds-number flows in three dimensional collapsible tubes. Journal of Fluid Mechanics, 486:79-103, 2003.

Heil, M. Stokes flow in collapsible tubes: computation and experiment. Journal of Fluid Mechanics, 353:285-312, 1997.

Heil, M. Stokes Flow in an Elastic Tube–Large-Displacement Fluid-Structure Interaction Problem. International Journal for Numerical Methods in Fluids, 28:243-265, 1998.

Heil, M. and Pedley, T. J. Large Post-Buckling Deformations of Cylindrical Shells Conveying Viscous Flows. Journal of Fluids and Structures, 10:565-599, 1996.

Holt, J. P. The collapse factor in the measurement of venous pressure: the flow of fluid through collapsible tubes. American Journal of Physiology, 134:292-299, 1941.

Holt, J. P. Flow of Liquids Through Collapsible Tubes. Circulation Research, VII: 342-353, 1959.

Jensen, O. E. and Pedley, T. J. The existence of steady flow in a collapsed tube. Journal of Fluid Mechanics, 206:339-374, 1989.

Kamm, R. D. and Pedley, T. J. Flow in Collapsible Tubes: A Brief Review. Transactions of the ASME Journal of Biomechanical Engineering, 111:177-179, 1989.

Katz, A. I., Chen, Y., and Moreno, A. H. Flow Through a Collapsible Tube. Biophysical Journal, 9:1261-1279, 1969.

Kececioglu, I., McClurken, M. E., Kamm, R. D., and Shapiro, A. H. Steady, supercritical flow in collapsible tubes. Part 1. Experimental observations. Journal of Fluid Mechanics, 109:367-389, 1981.

Kozlovsky, P., Zaretskya,U., Jaffab, A. J. and Elad, D. General tube law for collapsible thin and thick-wall tubes. Journal of Biomechanics 47:2378–2384, 2014.

Knowlton, F. P. and Starling, E. H. The influence of variations in temperature and blood pressure on the performance of the isolated mammalian heart. Journal of Physiology-London, 44:206-219, 1912.

Kresch, E. and Noordergraaf, A. Cross-Sectional Shape of Collapsible Tubes. Biophysical Journal, 12:274-294, 1972.

Lyon, C. K., Scott, J. B., and Wang, C. Y. Flow through collapsible tubes at low Reynolds numbers. Applicability of the waterfall model. Circulation Research, 47:68-73, 1980.

Marzo, A., Luo, X. Y., and Bertram, C. D. Three-dimensional collapse and steady flow in thick-walled flexible tubes. Journal of Fluids and Structures, 20:817-835, 2005.

Meng, Y., Rao, M. A., and Dutta, A. K. Computer Simulation of the Pharyngeal Bolus Transport of Newtonian and Non-Newtonian Fluids. Trans. I. Chem.E. Part C: Food & Bioproducts Processing, 83:297-305, 2005.

Nahar, S., Jeelani, S. A. K., and Windhab, E. J. Influence of elastic tube deformation on flow behavior of a shear thinning fluid. Chemical Engineering Science, 75:445-455, 2012a.

Nahar, S., Jeelani, S. A. K., Windhab, E. J. Peristaltic flow characterization of a shear thinning fluid through an elastic tube by UVP. Applied Rheology, 22 (4), 43941, 2012b.

Nahar, S., Jeelani, S. A. K., Windhab, E. J. Prediction of velocity profiles of shear thinning fluids flowing in elastic tubes. Chemical Engineering Communication, 200 (6), 820-835, 2013.

Neelamegam, R. and Shankar, V. Experimental study of the instability of laminar flow in a tube with deformable walls. Physics of Fluids, 27 (2): 024102: 1-18, 2015.

Pedley, T. J. The Fluid Mechanics of Large Blood Vessels. Cambridge University Press, Cambridge, 1980.

Raj, K. M., Chakraborty, J., Gupta, S. D., and Chakraborty; S. Flow-induced deformation in a microchannel with a non-Newtonian fluid. Biomicrofluidics, 12: 034116, 2018.

Roser, M. E. and Peskin, C. S. Fluid Flow in Collapsible Elastic Tubes: A Three-Dimensional Numerical Model. New York Journal of Mathematics, 7:281-302, 2001.

Rosmery, W., Pedley, T. J., and Riley, D. S. Viscous flow in collapsible tubes of slowly varying elliptical cross-section. Journal of Fluid Mechanics, 81:273-294, 1977.

Scroggs, R. A., Beck, S. B. M., and Patterson, E. A. An Integrated Approach to Modelling the Fluid-Structure Interaction of a Collapsible Tube. JSME International Journal, 47:20-28, 2004.

Rana, J., and Murthy, P. V. S. N. Unsteady solute dispersion in Herschel-Bulkley fluid in a tube with wall absorption, Physics of Fluids 28, 111903, 2016.

Shapiro, A. H., Jaffrin, M. Y., and Weinberg, S. L. Peristaltic pumping with long wavelengths at low Reynolds number. *Journal of Fluid Mechanics*, 37:799-825, 1969.

Shapiro, A. H. Physiologic and medical aspects of flow in collapsible tubes. Proc. 6th Canad. Congr. Appl. Mech., Van- couver, pages 883-905, 1977a.

Shapiro, A. H. Steady Flow in Collapsible Tubes. Transactions of the ASME Journal of Biomechanical Engineering, 99:126-147, 1977b.

Tanner, F. X., Al-Habahbeh, A. A., Feigl, K. A., Nahar, S., Jeelani, S. A. K., Case, W. R., and Windhab, E. J. Numerical and Experimental Investigation of a Non- Newtonian Flow in a Collapsed Elastic Tube. Applied Rheology, 22:63910, 2012.

Unhale, S. A., Marino, G., and Parameswaran, S. A One Dimensional Model to Predict Steady Flow Through a Collapsible Tube. International Journal for Computational Methods in Engineering Science and Mechanics, 6:95-103, 2005.

Whittaker, R. J., Heil, M., Jensen, O. E., and Waters, S. L. A rational Derivation of a Tube Law from Shell Theory. The Quarterly Journal of Mechanics and Applied Mathematics, 63:465–496, 2010.

Wyk, S. V., Wittberg, L. P., Bulusu, K. V., Fuchs, L., and Plesniak, M. W. Non-Newtonian perspectives on pulsatile blood-analog flows in a 180° curved artery model, Physics of Fluids 27, 071901, 2015.

Zhu, J. and Wang, X. A study of steady and unsteady flow in a collapsible channel. Computational Fluid and Solid Mechanics, pages 1597-1600, 2003.
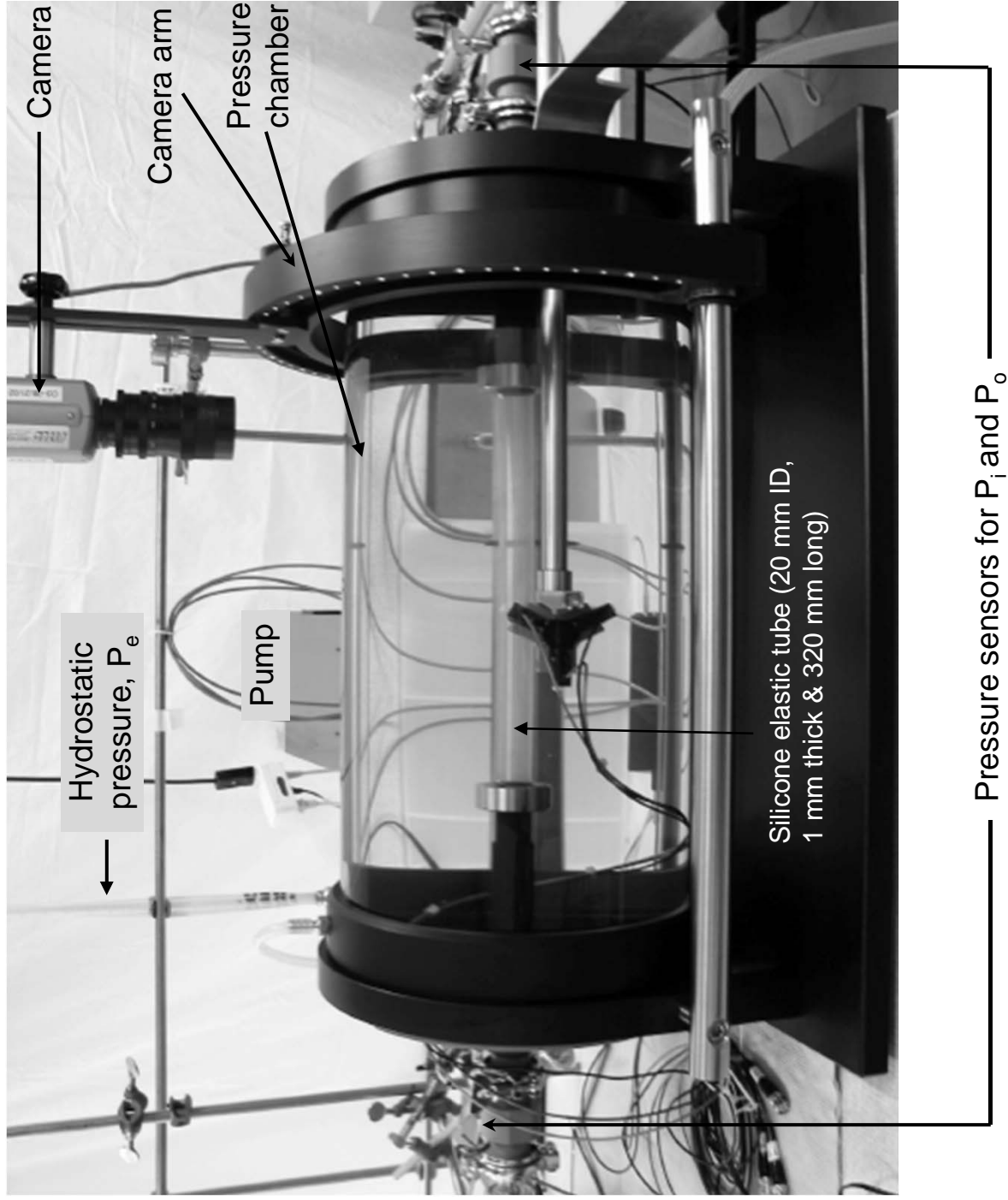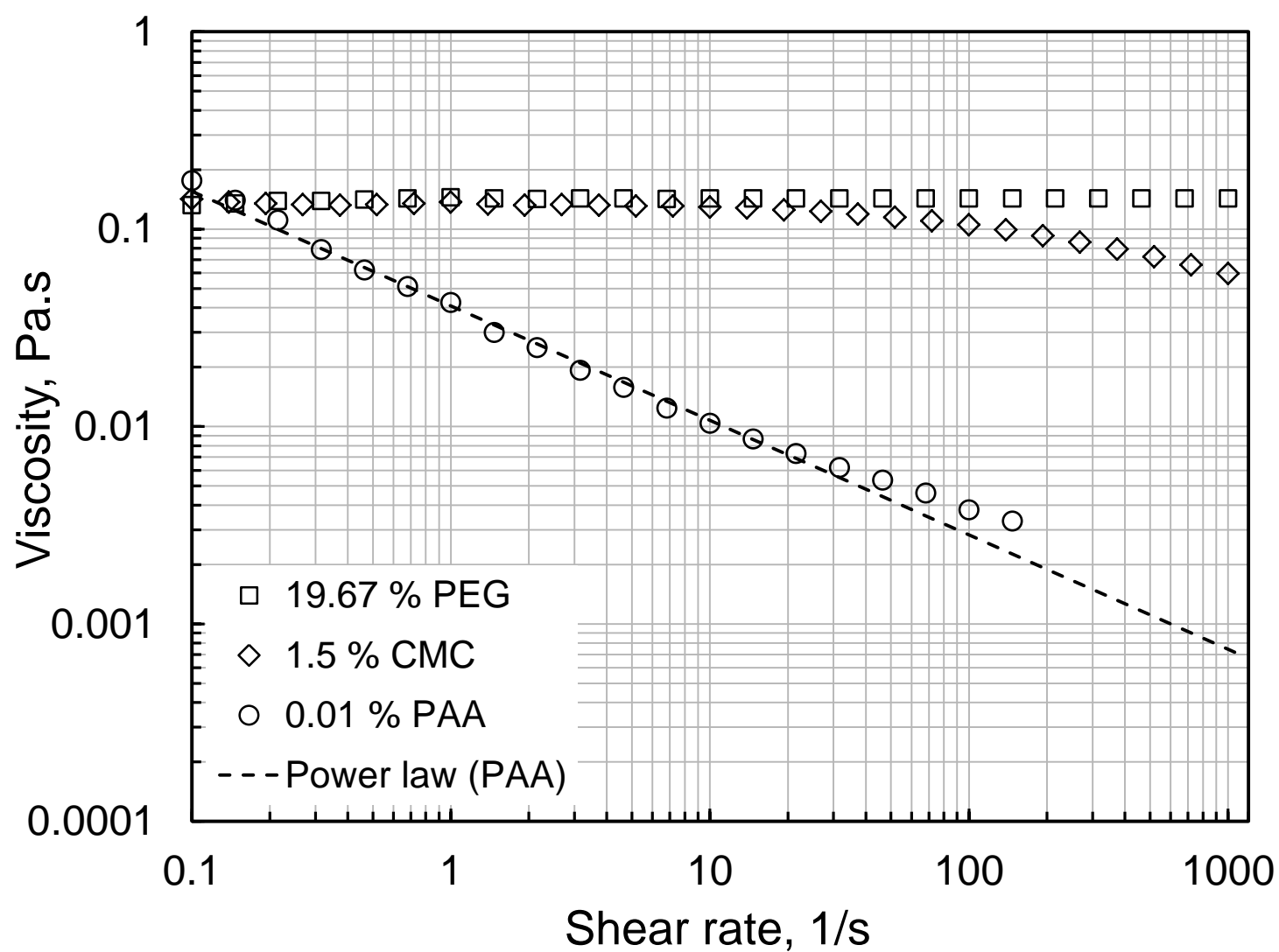
Figure (b): Storage and loss modulus (Pa) as a function of Frequency (rad/s) for 0.01 % PAA. Legend: ◇ G' (0.01 % PAA), ◆ G" (0.01 % PAA).

Physics of Fluids

Tube shapes

PEG

CMC

PAA

Channel [-]

Flow velocity, m/s

P_e = 125 mbar
P_{tm} = - 29.31 mbar

P_e = 120 mbar
P_e = - 23.17 mbar

P_e = 100 mbar
P_e = 10.59 mbar

P_e = 18 mbar
P_{tm} = 92.39 mbar

P_e = 105 mbar
P_{tm} = - 17.69 mbar

P_e = 100 mbar
P_{tm} = - 13.02 mbar

P_e = 90 mbar
P_{tm} = - 2.62 mbar

P_e = 18 mbar
P_{tm} = 78.69 mbar

P_e = 105 mbar
P_{tm} = - 18.85 mbar

P_e = 100 mbar
P_{tm} = - 13.89 mbar

P_e = 90 mbar
P_{tm} = - 3.68 mbar

P_e = 18 mbar
P_{tm} = 68.55 mbar

Channel (-)

Flow velocity (m/s)

(a) PEG

(b) CMC

Legend:
- Pe=18 mbar
- Pe=85 mbar
- Pe= 90 mbar
- Pe=93 mbar
- Pe=97 mbar
- Pe=100 mbar
- Pe=105 mbar
- Pe=110 mbar
- Pe=120 mbar

Axis labels: $\Delta P = P_i - P_o$ in mbar (vertical), Flow rate, Q ml/s (horizontal)

$P_{tm} = -37$ mbar
$P_{tm} = -33$ mbar
$P_{tm} = -29$ mbar
$P_{tm} = -23$ mbar

above critical P_e
below critical P_e

$P_e = 120$ mbar
$P_e = 110$ mbar
$P_e = 105$ mbar
$P_e = 100$ mbar
$P_e = 97$ mbar
$P_e = 90$ mbar
$P_e = 18$ mbar

(c) PAA